# Nonlinear pulse compression to 22 fs at 15.6 µJ by an all-solid-state multipass approach

EDOARDO VICENTINI,[1,2] YUCHEN WANG,[2] DAVIDE GATTI,[1,2] ALESSIO GAMBETTA,[1,2] PAOLO LAPORTA,[1,2] GIANLUCA GALZERANO,[1,2] KELLY CURTIS,[3] KENNETH MCEWAN,[3] CHRISTOPHER R. HOWLE,[3] AND NICOLA COLUCCELLI[1,2,*]

[1]*Dipartimento di Fisica - Politecnico di Milano, Piazza Leonardo da Vinci 32, 20133 Milano, Italy*
[2]*Istituto di Fotonica e Nanotecnologie - CNR, Piazza Leonardo da Vinci 32, 20133 Milano, Italy*
[3]*Defence Science and Technology Laboratory, Porton Down, Salisbury SP4 0JQ, UK*
[*]*nicola.coluccelli@polimi.it*

**Abstract:** We demonstrate nonlinear compression of pulses at 1.03 µm and repetition rate of 200 kHz generated by a ytterbium fiber laser using two cascaded all-solid-state multipass cells. The pulse duration has been compressed from 460 to 22 fs, corresponding to a compression factor of ~21. The compressed pulse energy is 15.6 µJ, corresponding to an average power of 3.1 W, and the overall transmission of the two compression stages is 76%. The output beam quality factor is $M^2$ ~1.2 and the excess intensity noise introduced by nonlinear broadening is below 0.05%. These results show that nonlinear pulse compression down to ultrashort durations can be achieved with an all-solid-state approach, at pulse energies much higher than previously reported, while preserving the spatial characteristics of the laser.

## 1. Introduction

High-energy ultrashort laser pulses are employed in a vast variety of scientific and technological applications, such as impulsive vibrational spectroscopy [1–3], time-resolved stimulated Raman spectroscopy [4–6], near-field imaging techniques [7], and generation of ultrashort terahertz radiation [8]. Besides these, standoff detection of chemical and biological warfare agents by broadband coherent anti-Stokes Raman spectroscopy also requires ultrashort high-energy laser pulses (ideally, pulse duration <20 fs and energy >10 µJ), to efficiently excite and detect vibrational coherences of remote samples [9–12]. To this purpose, Ti:sapphire (Ti:Sa) amplifier systems have been used till now due to the large bandwidth enabled by Ti:Sa gain materials, however, besides the high-complexity and large footprint typical of these systems, they are operated at low repetition rates of 1 kHz due to the constraints of system architecture. Alternatively, the current generation of femtosecond ytterbium-fiber lasers provide easy access to repetition rates higher than 100 kHz, beneficial for increasing the Raman signal detected over a specified integration time (or improving the acquisition rate), and are characterized by a rugged and compact architecture, though the pulse durations are inherently limited to a few hundreds of femtoseconds in these lasers due to the narrow gain bandwidth as compared to Ti:Sa systems. Therefore, it is necessary to compress the pulses to shorter durations in order that ytterbium (Yb) lasers become a viable replacement of Ti:Sa systems in ultrafast applications. External nonlinear pulse compression allows combination of the high pulse energy of Yb-based lasers with short pulse durations. The compression relies on nonlinear spectral broadening via self-phase modulation by the Kerr effect and subsequent chirp removal. There have been several reports on the compression of Yb laser pulses based on different setups and nonlinear media depending on the pulse energies and peak powers of interest. Nonlinear pulse compression within dielectric waveguides [13,14] (typically, solid-core fused-silica fibers) can easily provide sub-20 fs pulse durations, however, it

is limited by the onset of catastrophic self-focusing which occurs at peak powers of a few MW, corresponding to typical maximum pulse energies at the μJ-level. Higher pulse energies can be handled using noble gases as the nonlinear medium, because of the much higher (three orders of magnitude) self-focusing threshold [15]. Gas-filled hollow-core capillaries [16,17] are used for nonlinear compression of pulses with energies exceeding 100 μJ (peak powers of over 1 GW) due to the limitations imposed by propagation losses which requires core diameter of capillaries larger than ~150 μm. In the 1-100 μJ range of energies the situation is less defined and different technical solutions are being developed and tested to fill the gap. One promising approach is based on using gas-filled Kagome hollow-core photonic crystal fibers (HC-PCF) [18,19], which allow for smaller diameters than capillaries and hence have been used to demonstrate nonlinear pulse compression down to ~30 fs with pulse energies of few tens of μJ. Recently, a new approach based on a multipass cell (MPC) for repeated propagation through a noble gas or a thin bulk nonlinear medium has been proposed for compression of intense femtosecond laser pulses; the first demonstration was based on an Innoslab laser [20]. When using a noble gas, besides the additional complexity represented by operation of a pressurized gas chamber, pulse energies are again limited to the range above 100 μJ to attain sufficient nonlinear spectral broadening, though very short pulse durations of 26.5 fs have been demonstrated in this case [21]. On the other hand, use of a thin bulk nonlinear medium allows the implementation of an all-solid-state setup which has proven effective to fill the gap in the 1-100 μJ range, with various combinations of reported pulse durations and energies (170 fs at 37.5 μJ [20], 115 fs at 7.5 μJ [22], 35 fs at 4.5 μJ [23], 88 fs at 8.3 μJ [24], 40 fs at 4.8 μJ [25]). Pulse compression down to 18 fs have been also demonstrated using cascaded stages of all-solid-state MPCs at a maximum pulse energy of 3.5 μJ, and overall efficiency and compression factor below 60% and 14.7, respectively [26,27].

In this paper, we report on a nonlinear pulse compression system based on all-solid-state MPCs generating ultrashort pulses at 1.03 μm with durations of 22 fs and maximum energy of 15.6 μJ. The system has a femtosecond Yb-fiber laser at the input and comprises two cascaded stages of MPCs for nonlinear broadening and compression of laser pulses. The overall efficiency and compression factor of the system are 76% and 21, respectively. The pulse durations and intensity stability have been characterized at the output of both stages. The output beam quality factor is $M^2$ ~1.2. These results show that the all-solid-state MPC approach for nonlinear pulse compression allows for a novel combination of short pulse duration and high energy of 22 fs and 15.6 μJ, respectively, with the highest compression factor of 21 reported so far. In addition, as it is based on only two cascaded stages, our setup has reduced complexity and footprint, and yields improved transmission efficiency.

## 2.  Experiment

The layout of the setup used for nonlinear pulse compression is shown in Fig. 1. The system starts with a commercial femtosecond Yb-fiber laser (Aeropulse-FS, NKT-Photonics) delivering laser pulses with a maximum energy of 20.5 μJ and a repetition frequency of 200 kHz (tunable to 1 MHz). Figure 2 shows the spectrum and autocorrelation trace of pulses as measured at the output of the Yb fiber laser; assuming Gaussian shaped pulses, the inferred pulse duration is 460 fs. The beam quality factors measured along the horizontal and vertical directions are $M_x^2$=1.10 and $M_y^2$=1.09, respectively. The beam is first passed through a proper mode-matching telescope and then coupled into the first stage of nonlinear broadening by means of a right-angle prism mirror with vertical aperture of 5 mm. Nonlinear broadening is implemented in a Herriott-type MPC, comprising two high-reflectivity mirrors (reflectivity > 99.9% from 900 to 1200 nm) with a diameter of 50.8 mm and a radius of curvature (ROC) of 300 mm, and an anti-reflection (AR) coated fused silica plate with a thickness of 9.5 mm placed in the center of the cell. The principle of operation of the MPC as a nonlinear pulse compression device is based on repeated steps of propagation between two curved mirrors and a nonlinear medium that induces a small

nonlinear phase shift at each step. Under these conditions, pulses with peak powers above the threshold for critical self-focusing can be spectrally broadened and beam quality degradation during propagation through the nonlinear medium is mitigated [20–22].

The MPC can be modelled as a spherical resonator with a relatively long Kerr lens inside using ABCD matrix formalism to calculate the "self-consistent" mode, i.e. the mode reproducing the same spot size and radius of curvature at each step of propagation within the MPC. In the first MPC, the distance between the two curved mirrors is set to 520 mm, corresponding to a near-concentric resonator design with calculated beam radius of 0.18 and 0.5 mm on the fused silica plate and curved mirrors, respectively, assuming a pure fundamental Gaussian mode. The beam quality of input pulses can be included by multiplying the calculated beam radii with the specified $M_x$ and $M_y$. The design of the first MPC resembles the characteristics of other near-concentric MPC setups reported elsewhere [20,22,23,26]. The telescope at the input of the MPC provides mode-matching of the laser beam to the calculated spot sizes, in order that the beam dimension inside the fused silica plate (and mirrors) at each following step is always the same; this ensures on one hand that each step of propagation contributes efficiently to induce nonlinear phase, and, on the other, that catastrophic self-focusing due to converging spot-sizes on subsequent steps is avoided. The net dispersion experienced by laser pulses at each step of propagation within the MPC is close to zero, a condition which puts the propagation in a regime of pure self-phase modulation (SPM); in particular, the group delay dispersion (GDD) around 1030 nm of the dielectric coating on the curved mirrors and of the fused silica plate in the
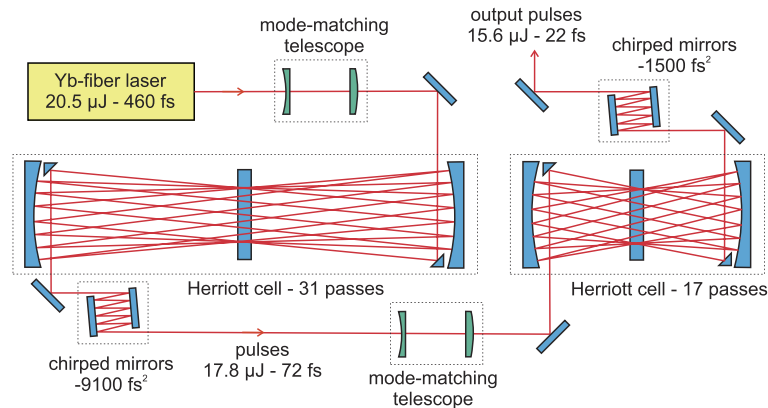


**Fig. 1.** Layout of the system for nonlinear pulse compression.
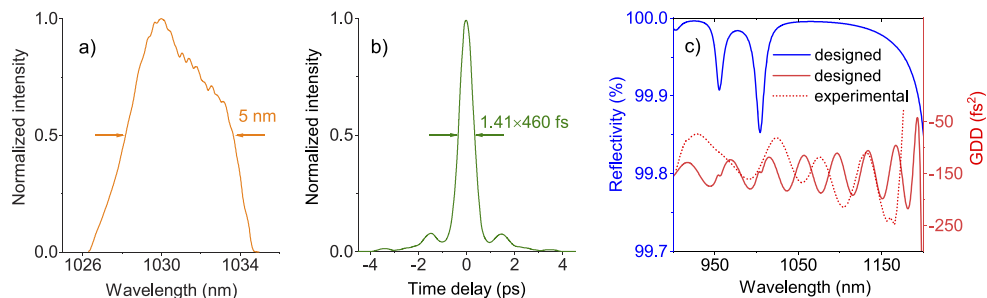


**Fig. 2.** a) Spectrum and b) autocorrelation trace of pulses at the output of the Yb laser. c) Reflectivity by design (blue), and group delay dispersions by design (solid red) and measured (dotted red) of the curved mirrors used for both MPC nonlinear compression stages.

center of the MPC are $-150\pm70$ fs$^2$ and $+170$ fs$^2$, respectively. Figure 2(c) shows the reflectivity (design) and GDD (design and measurement) of the curved mirrros. The beam is extracted from the MPC by a second right-angle prism mirror and collimated by a lens with focal length of 300 mm. The MPC and the input beam are aligned to form a circle of 16 evenly spaced reflections on each curved mirror (one of which is intercepted by the input/output right-angle prism mirrors). This yields 31 passes through the nonlinear element. The spectrally broadened pulses are sent through a chirped mirror compressor with a total GDD of $-9100$ fs$^2$ (16 reflections on 2 mirrors with GDD of $-500$ fs$^2$ and 2 reflections on 2 mirror with GDD of $-550$ fs$^2$.). Figure 3 shows the pulse energy and transmission efficiency as a function of the power level as measured at the output of the first broadening/compression stage. A modest roll-off of the energy characteristic is observed at the highest operative levels corresponding to a slight reduction of transmission efficiency from 88.2% to 86.8%; this is ascribed to slightly increasing losses from the AR-coating of the fused silica plate as the spectrum of pulses is broadened. The maximum pulse energy at the output of the first stage is 17.8 µJ.
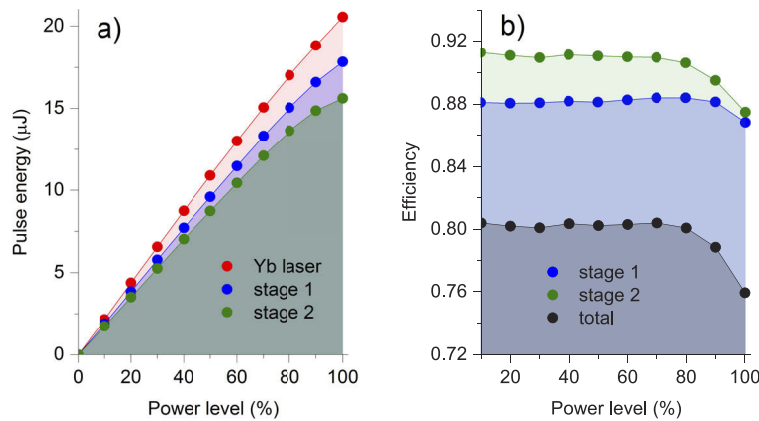


**Fig. 3.** a) Pulse energy at the output of the Yb laser, and the two broadening/compression stages. b) Input/output efficiency of each broadening/compression stage and overall efficiency of the two cascaded stages.

The laser pulses at the output of the first stage have been characterized in the time and frequency domain by second-harmonic frequency resolved optical gating (SH-FROG) analysis, and the results are shown in Fig. 4. The spectrum is broadened to a $-3$ dB bandwidth of 30 nm, while the pulse is compressed to 72 fs, close to the Fourier-transform limit (FTL) of 67 fs. Taking into account the original pulse duration of 460 fs at the output of the Yb-fiber laser, this corresponds to a compression factor of 6.4 in the first nonlinear compression stage. The residual positive quadratic phase of the spectrum in Fig. 4(d) is ascribed to sub-optimal compensation of pulse dispersion by the chirped mirror compressor (each reflection onto the chirped mirror provides a discrete GDD contribution of $\sim-500$ fs$^2$).

A second stage of nonlinear compression has been cascaded to the first in order to generate more bandwidth and hence further reduce the pulse duration. The second MPC consists again of two curved mirrors with a diameter of 50.8 mm and ROC of 300 mm and a fused silica plate with a thickness of 9.5 mm, however, instead of using a near-concentric design, a near-confocal configuration with a distance between mirrors set to 250 mm has been adopted in this case. This approach is required by the higher peak power at the input of the second MPC, as the near-confocal configuration provides larger calculated beam radius of 0.22 mm (fundamental Gaussian mode) at the cavity focus, and hence reduces peak intensity on the fused silica plate to avoid catastrophic self-focusing. Mode-matching is again achieved with a telescope at the input
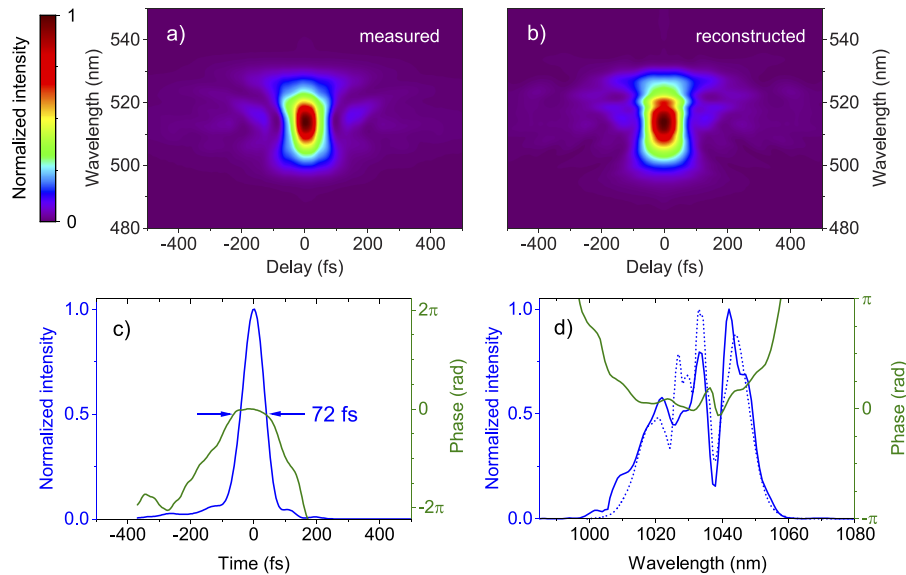
**Fig. 4.** Temporal characterization of laser pulses at the output of the first broadening/compression stage at full power. a) measured SHG-FROG trace, and b) reconstructed FROG trace with 0.007 error on a $512 \times 512$ grid. c) temporal intensity and phase. d) reconstructed (solid) and measured (dotted) spectral intensity and phase.

of the second MPC. The net GDD of the cavity mirrors and fused silica plate (air contribution can be neglected) around 1030 nm is again close to zero, however, it's worth noting that the GDD of mirror coatings exhibits larger oscillations for spectral components far from the design wavelength of 1030 nm. The second MPC is set to form a circle of 9 evenly spaced reflections on each curved mirror, yielding 17 passes through the nonlinear element. The output beam is collimated with a lens with 150-mm focal length and then sent through a chirped mirror compressor with a total GDD of $-1500$ fs$^2$ (10 reflections on 2 mirrors with GDD of $-150$ fs$^2$). As shown in Fig. 3, the energy characteristic of the pulses at the output of the second nonlinear compression stage has a more pronounced roll-off, which results from the variation of transmission efficiency from 91.0 to 87.5%; this is ascribed to the reduced performance of the fused silica plate AR coating (V-coating at 1030 nm) as the spectrum gets broadened far from the design wavelength of 1030 nm. The maximum energy of the pulses at the output of the second nonlinear compression stage is 15.6 μJ, corresponding to an overall transmission of 76% for the two cascaded stages. The reported efficiency is already competitive to that of Kagome HC-PCF, and could be readily improved by the adoption of a fused silica plate with broader AR coating. Figure 5 shows the results of SH-FROG analysis performed on pulses at the output of the system. The spectral broadening induced by the second MPC generates components from 950 to 1180 nm (measured with Yokogawa AQ6370AD), and the measured compressed pulse duration is 22 fs, corresponding to 6.4 optical cycles at a central wavelength of 1030 nm. The presence of some pedestals in the temporal profile of the pulse is ascribed to the oscillations of GDD from the dielectric mirror coatings experienced by the ultra-broad spectrum generated at maximum pulse energy. This is also confirmed by calculation of the FTL at a pulse duration of 15 fs that could in principle be obtained with optimal GDD compensation of the generated spectrum. Around 57% of the pulse energy resides in the main peak of the pulse temporal envelope, corresponding to an estimated output peak power of ~400 MW. The pulse peak power and intensity at the input of the second MPC are estimated to be ~247 MW and ~160 GW/cm$^2$, corresponding to a calculated

B-integral [28](nonlinear phase) of $0.6\pi$ per pass and $10.2\pi$ over all 17 passes within the MPC, however, this is an overestimate of the B-integral as it does not take into account pulse dispersion. An approximate measurement of the overall B-integral experienced by the pulse can be obtained by the number of peaks in the spectrum observed at the output of the second MPC (see Fig. 5(d)), that is equal to 7. The B-integral is then obtained as $(7\text{-}0.5)\pi=6.5\pi$ [28], corresponding to $\sim0.4\pi$ per pass, which is consistent with the overestimate value given before reduced by the effect of dispersion which increases the pulse duration (reduce the peak intensity) as the pulse propagates within the MPC.
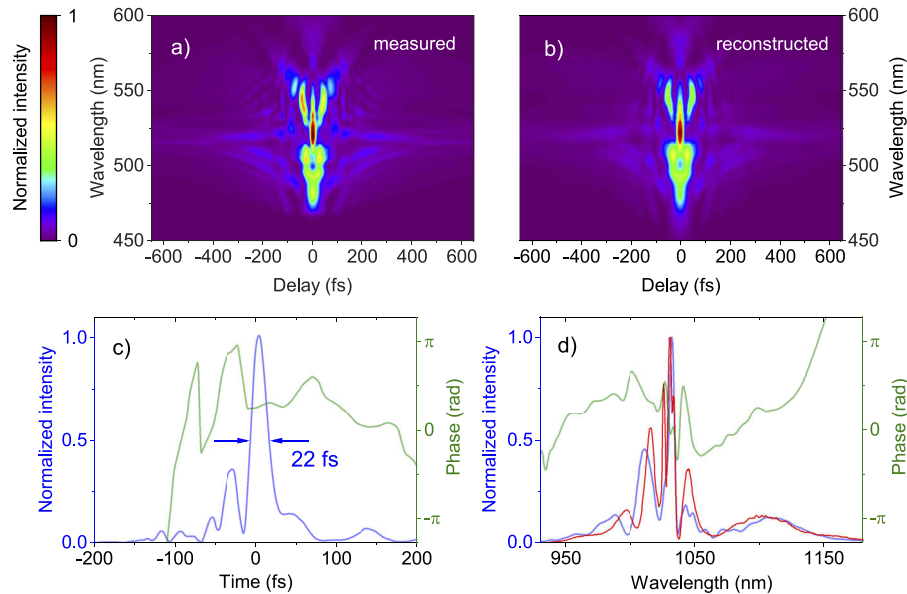


**Fig. 5.** Temporal characterization of laser pulses at the output of the second broadening/compression stage at full power. a) measured SHG-FROG trace, and b) reconstructed FROG trace with 0.003 error on a $512 \times 512$ grid. c) temporal intensity and phase. d) reconstructed (blue) and measured (red) spectral intensity and phase (green)

Figure 6 shows the measurement of beam diameters along the caustic generated by a focusing lens, according to the d4$\sigma$ definition required by ISO 11670 standard, at the output of the system at maximum pulse energy. The fit to the beam caustic provides the measurement of beam quality factors $M_x^2=1.21$ and $M_y^2=1.18$. As the beam quality factors measured at the input of the MPC setup are $M_x^2=1.10$ and $M_y^2=1.09$, it can be inferred that the spatial coherence of the beam is only slightly affected by the nonlinear compression stages. The slight increase of the beam quality factors at the output of the second MPC indicates that the B-integral value per pass of $\sim 0.4\pi$ is at the limit of what can be done using this setup to preserve the homogeneity of spectral broadening across the beam profile.

Finally, the intensity stability of the laser pulses at the output of the Yb-laser and the two nonlinear compression stages has been characterized at maximum energy by relative intensity noise (RIN) analysis. The results are shown in Fig. 7, where the power spectral density of noise has been characterized till the Fourier frequency of 100 kHz to remove the replicas at harmonics of the repetition rate (200 kHz). Overall, the RIN spectra at the output of the two nonlinear compression stages closely resembles the RIN of the Yb-fiber laser over all the spectral range analysed, apart from a minor degradation. The resulting integrated noise from 100 kHz down to a few Hz at the output of the system amounts to 0.34%, compared with 0.3% measured at the
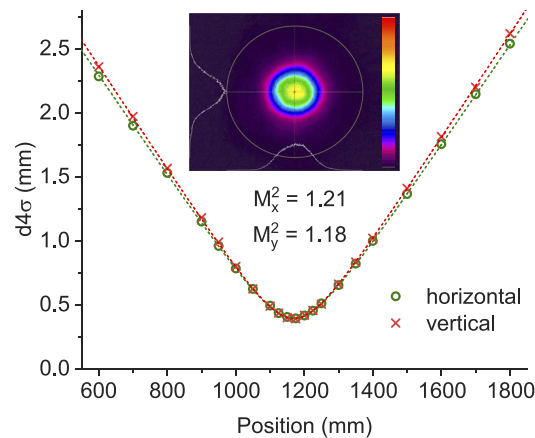
**Fig. 6.** Beam quality measurement based on d4$\sigma$ definition of beam diameter along the horizontal (green) and vertical (red) plane. The inset shows the near-field beam profile at the output of the second multipass cell.

output of the Yb-fiber laser. This result confirms that the intensity stability of laser pulses is substantially preserved even at the high nonlinear compression factor and energy obtained with the all-solid-state setup presented here.
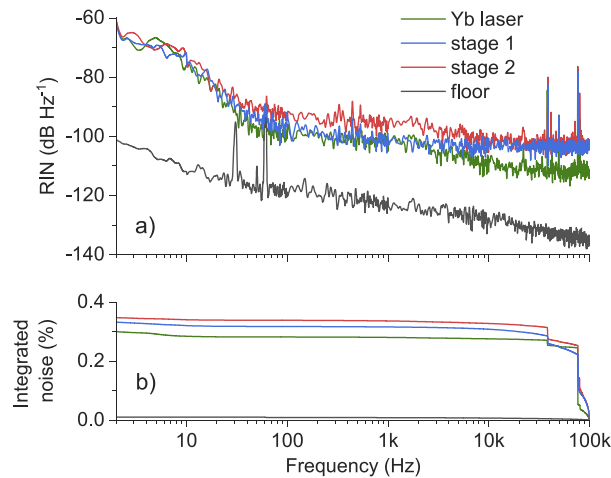


**Fig. 7.** a) Relative intensity noise spectrum of the Yb laser, the two broadening/compression stages, and the detector noise floor, and b) corresponding integrated intensity noise from 2 Hz to 100 kHz.

## 3. Conclusion

In conclusion, we demonstrated an all-solid-state setup for nonlinear compression of laser pulses based on two cascaded MPCs. The pulses at the output of a commercial Yb-fiber laser have been compressed to a duration of 22 fs, with an overall nonlinear compression factor of 21, at a maximum pulse energy of 15.6 µJ. The transmission efficiency of the cascaded system is 76% with an excellent output beam quality factor of ~1.2. The current limit to the output pulse energy is set by the maximum energy attainable from the Yb-fiber laser adopted here, and further

extension to higher pulse energy should be investigated, even though no fundamental limits to performance scaling is envisaged, provided that a proper MPC design is implemented to avoid detrimental effects of Kerr self-focusing. The results reported here show that the approach to nonlinear compression of laser pulses by all-solid-state setups can be safely scaled to pulse energy levels above 10 μJ while synthesizing pulses with ultrashort durations.

## Funding

## Disclosures

The authors declare no conflicts of interest.

## References

1. D. Polli, M. R. Antognazza, D. Brida, G. Lanzani, G. Cerullo, and S. De Silvestri, "Broadband pump-probe spectroscopy with sub-10-fs resolution for probing ultrafast internal conversion and coherent phonons in carotenoids," Chem. Phys. **350**(1-3), 45–55 (2008).
2. M. Liebel, C. Schnedermann, T. Wende, and P. Kukura, "Principles and applications of broadband impulsive vibrational spectroscopy," J. Phys. Chem. A **119**(36), 9506–9517 (2015).
3. J. Du, J. Harra, M. Virkki, J. M. Makela, Y. Leng, M. Kauranen, and T. Kobayashi, "Surface-Enhanced Impulsive Coherent Vibrational Spectroscopy," Sci. Rep. **6**(1), 36471 (2016).
4. P. Kukura, D. W. McCamant, and R. A. Mathies, "Femtosecond stimulated Raman spectroscopy," Annu. Rev. Phys. Chem. **58**(1), 461–488 (2007).
5. H. Kuramochi, S. Takeuchi, and T. Tahara, "Femtosecond time-resolved impulsive stimulated Raman spectroscopy using sub-7-fs pulses: Apparatus and applications," Rev. Sci. Instrum. **87**(4), 043107 (2016).
6. D. R. Dietze and R. A. Mathies, "Femtosecond stimulated Raman spectroscopy," ChemPhysChem **17**(9), 1224–1251 (2016).
7. Y. Nishiyama, K. Imura, and H. Okamoto, "Observation of plasmon wave packet motions via femtosecond time-resolved near-field imaging techniques," Nano Lett. **15**(11), 7657–7665 (2015).
8. J. Darmo, T. Müller, W. Parz, J. Kröll, G. Strasser, and K. Unterrainer, "Few-cycle terahertz generation and spectroscopy of nanostructures," Philos. Trans. R. Soc., A **362**(1815), 251–262 (2003).
9. M. T. Bremer, P. J. Wrzesinski, N. Butcher, V. V. Lozovoy, and M. Dantus, "Highly selective standoff detection and imaging of trace chemicals in a complex background using single-beam coherent anti-Stokes Raman scattering," Appl. Phys. Lett. **99**(10), 101109 (2011).
10. M. T. Bremer, P. J. Wrzesinski, N. Butcher, V. V. Lozovoy, and M. Dantus, "Standoff and arms-length detection of chemicals with single-beam coherent anti-Stokes Raman scattering," Appl. Opt. **48**(4), B17–B22 (2009).
11. O. Katz, A. Natan, Y. Silberberg, and S. Rosenwaks, "Standoff detection of trace amounts of solids by nonlinear Raman spectroscopy using shaped femtosecond pulses," Appl. Phys. Lett. **92**(17), 171116 (2008).
12. D. Pestov, X. Wang, G. O. Ariunbold, R. K. Murawski, V. A. Sautenkov, A. Dogariu, A. V. Sokolov, and M. O. Scully, "Single-shot detection of bacterial endospores via coherent Raman spectroscopy," Proc. Natl. Acad. Sci. U. S. A. **105**(2), 422–427 (2008).
13. O. Pronin, M. Seidel, F. Lücking, J. Brons, E. Fedulova, M. Trubetskov, V. Pervak, A. Apolonski, T. Udem, and F. Krausz, "High-power multi-megahertz source of waveform-stabilized few-cycle light," Nat. Commun. **6**(1), 6988 (2015).
14. H. Carstens, M. Högner, T. Saule, S. Holzberger, N. Lilienfein, A. Guggenmos, C. Jocher, T. Eidam, D. Esser, V. Tosa, V. Pervak, J. Limpert, A. Tünnermann, U. Kleineberg, F. Krausz, and I. Pupeza, "High-harmonic generation at 250 MHz with photon energies exceeding 100 eV," Optica **3**(4), 366–369 (2016).
15. E. Haddad, R. Safaei, A. Leblanc, R. Piccoli, Y. Jeong, H. Ibrahim, B. E. Schmidt, R. Morandotti, L. Razzari, F. Légaré, and P. Lassonde, "Molecular gases for pulse compression in hollow core fibers," Opt. Express **26**(19), 25426–25436 (2018).
16. S. Hädrich, A. Klenke, A. Hoffmann, T. Eidam, T. Gottschall, J. Rothhardt, J. Limpert, and A. Tünnermann, "Nonlinear compression to sub-30-fs, 0.5 mJ pulses at 135 W of average power," Opt. Lett. **38**(19), 3866–3869 (2013).
17. L. Lavenu, M. Natile, F. Guichard, Y. Zaouter, M. Hanna, E. Mottay, and P. Georges, "High-energy few-cycle Yb-doped fiber amplifier source based on a single nonlinear compression stage," Opt. Express **25**(7), 7530–7537 (2017).
18. F. Guichard, A. Giree, Y. Zaouter, M. Hanna, G. Machinet, B. Debord, F. Gérôme, P. Dupriez, F. Druon, C. Hönninger, E. Mottay, F. Benabid, and P. Georges, "Nonlinear compression of high energy fiber amplifier pulses in air-filled hypocycloid-core Kagome fiber," Opt. Express **23**(6), 7416–7423 (2015).

19. F. Emaury, C. J. Saraceno, B. Debord, D. Ghosh, A. Diebold, F. Gérôme, T. Südmeyer, F. Benabid, and U. Keller, "Efficient spectral broadening in the 100-W average power regime using gas-filled kagome HC-PCF and pulse compression," Opt. Lett. **39**(24), 6843–6846 (2014).

20. J. Schulte, T. Sartorius, J. Weitenberg, A. Vernaleken, and P. Russbüldt, "Nonlinear pulse compression in a multi-pass cell," Opt. Lett. **41**(19), 4511–4514 (2016).

21. P. Russbüldt, J. Weitenberg, J. Schulte, R. Meyer, C. Meinhardt, H. D. Hoffmann, and R. Poprawe, "Scalable 30 fs laser source with 530 W average power," Opt. Lett. **44**(21), 5222–5225 (2019).

22. J. Weitenberg, A. Vernaleken, J. Schulte, A. Ozawa, T. Sartorius, V. Pervak, H. Hoffmann, T. Udem, P. Russbüldt, and T. W. Hänsch, "Multi-pass-cell-based nonlinear pulse compression to 115 fs at 7.5 μJ pulse energy and 300 W average power," Opt. Express **25**(17), 20502–20510 (2017).

23. J. Weitenberg, T. Saule, J. Schulte, and P. Russbüldt, "Nonlinear pulse compression to sub-40 fs at 4.5 μJ pulse energy by multi-pass-cell spectral broadening," IEEE J. Quantum Electron. **53**(6), 1–4 (2017).

24. F. Meyer, N. Hekmat, T. Vogel, A. Omar, S. Mansourzadeh, F. Fobbe, M. Hoffmann, Y. Wang, and C. J. Saraceno, "Milliwatt-class broadband THz source driven by a 112 W, sub-100 fs thin-disk laser," Opt. Express **27**(21), 30340–30349 (2019).

25. S. Gröbmeyer, J. B. M. Seidel, and O. Pronin, "Laser Stabilization: Carrier-Envelope-Offset Frequency Stable 100-W Level Femtosecond Thin-Disk Oscillator," Laser Photonics Rev. **13**(3), 1800256 (2019).

26. K. Fritsch, M. Poetzlberger, V. Pervak, J. Brons, and O. Pronin, "All-solid-state multipass spectral broadening to sub-20 fs," Opt. Lett. **43**(19), 4643–4646 (2018).

27. G. Barbiero, R. N. Ahmad, H. Wang, F. Köttig, D. Novoa, F. Tani, J. Brons, P. J. Russell, F. Krausz, and H. Fattahi, "Towards 45 watt single-cycle pulses from Yb:YAG thin-disk oscillators," *2019 Conf. on Lasers Electro-Optics Eur. Eur. Quantum Electron. Conf. OSA Technical Digest* (Optical Society of America, 2019), paper cf_1_2.

28. G. P. Agrawal, *Nonlinear Fiber Optics* (Academic Press, 2001), Chap. 4.